SAND2021-0205

SANDIA REPORT

SAND2020
Printed Click to enter a date

Sandia National Laboratories

Hotel Room Computational Fluid Dynamics to Investigate Airborne Pathogen Dispersal Patterns

Rodriguez, Sal

Prepared by
Sandia National Laboratories
Albuquerque, New Mexico
87185 and Livermore,
California 94550

Issued by Sandia National Laboratories, operated for the United States Department of Energy by National Technology & Engineering Solutions of Sandia, LLC.

Available to DOE and DOE contractors from
U.S. Department of Energy
Office of Scientific and Technical Information
P.O. Box 62
Oak Ridge, TN 37831

Telephone: (865) 576-8401
Facsimile: (865) 576-5728
E-Mail: reports@osti.gov
Online ordering: http://www.osti.gov/scitech

Available to the public from
U.S. Department of Commerce
National Technical Information Service
5301 Shawnee Rd
Alexandria, VA 22312

Telephone: (800) 553-6847
Facsimile: (703) 605-6900
E-Mail: orders@ntis.gov
Online order: https://classic.ntis.gov/help/order-methods/

ABSTRACT

A hotel room unit consisting of a bedroom and bathroom was modelled using computational fluid dynamics (CFD) to investigate airborne pathogen dispersal patterns. The full-scale model includes a 'typical' hotel room configuration, furniture, and vents. The air sources and sinks include a bathroom vent, a heating, ventilation, and cooling (HVAC) unit located in the bedroom, and a ½" gap at the bottom of the entry door. In addition, the entry door and window can be opened or closed, as desired.

Three key configuration simulations were conducted: 1) both the bathroom vent and HVAC were on, 2) only the HVAC was on, and 3) only the bathroom vent was on. *If the HVAC air is from a fresh, clean source, or passes through a high-efficiency filter/UV device, then the first configuration is the safest, as contaminated air is highly reduced. The second configuration is also safe, but does not benefit from the outsourcing of potentially-infected air, such as contaminated air flowing through an ineffective filter. The third configuration should be avoided, as the bathroom vent causes air to flow from the hallway, which can be of dubious origin.*

The CFD simulations also showed that recirculation and swirling regions tend to accumulate the largest concentrations of heavier airborne particles, pathogens, dust, etc. These regions are associated with the largest turbulence kinetic energy (TKE) , and tend to occur in areas with flow recirculation and corners. Therefore, TKE presents a reasonable metric to guide the strategic location of pathogen mitigation devices.

The simulations show complex flow patterns with distinct upper and lower flow regions, swirling flow, and significant levels of turbulent mixing. These simulations provide intriguing insights that can be applied to help mitigate pathogen aerosol dispersal, generate building design guidelines, as well as provide insights for the strategic placement of mitigation devices, such as ultraviolet (UV) light, supplemental fans, and filters.

This page left blank

CONTENTS

1. Introduction 7
2. hotel room model 8
3. computational fluid dynamics simulations 12
   3.1. Simulation with Both HVAC and Bathroom Vents On 13
   3.2. Simulation with Only the HVAC Vent On 24
   3.3. Simulation with Only the Bathroom Vents On 25
4. Summary, Key Findings and recommendations, and suggestions for future work 27

LIST OF FIGURES

Figure 2-1. Hotel room floor plan. 8
Figure 2-2. Top view of CFD hotel room model. 9
Figure 2-3. Southwestern view of CFD hotel room model 9
Figure 2-4. Southeastern view of CFD hotel room model. 10
Figure 3-1. Velocity distribution at 0 s—Event Initiation. 14
Figure 3-2. Velocity distribution at 15 s (HVAC flow reaches door gap). 14
Figure 3-3. Velocity distribution at 30 s (the rooms reach a pseudo steady state). 15
Figure 3-4. Velocity distribution at 45 s (flow oscillates about mean from 45 to 120 s). 15
Figure 3-5. Velocity distribution at 60 s. 16
Figure 3-6. Velocity distribution at 75 s. 16
Figure 3-7. Velocity distribution at 90 s. 17
Figure 3-8. Velocity distribution at 105 s. 17
Figure 3-9. Velocity distribution at 120 s. 18
Figure 3-10. Velocity distribution at 120 s—southwestern view. 19
Figure 3-11. Velocity distribution at 120 s—northwestern view. 20
Figure 3-12. Velocity distribution at 120 s using arrows—southwestern view. 20
Figure 3-13. Velocity distribution at 120 s using arrows—southeastern view. 21
Figure 3-14. Normalized TKE at 30 s. 22
Figure 3-15. Normalized TKE at 60 s. 22
Figure 3-16. Normalized TKE at 90 s. 23
Figure 3-17. Normalized TKE at 120 s. 23
Figure 3-18. Velocity distribution at 120 s—only the HVAC is on; top view. 24
Figure 3-19. Velocity distribution at 120 s—only the HVAC is on; southwestern view. 25
Figure 3-20. Velocity distribution at 120 s—only the bathroom vent is on; top view. 26
Figure 3-21. Velocity distribution at 120 s—only the bathroom vent is on; southwestern view. 26

ACRONYMS AND DEFINITIONS

Abbreviation	Definition
A	flow area
CFD	computational fluid dynamics
g	gravitational constant
Gr	Grashof number (a measure of natural convection)
h	height
HVAC	heating, ventilation, and cooling
LES	large eddy simulation
LHS	left hand side
$\dot{m}$	mass flow rate
Nu	Nusselt number (a measure of natural convection)
Pr	Prandtl number (the ratio of the fluid viscous vs. thermal properties)
Ra	Rayleigh number (a measure of natural circulation that includes *Pr*)
Re	Reynolds number (a measure of the forced circulation)
RHS	right hand side
T	temperature
TKE	total kinetic energy (a measure of turbulence)
u	fluid velocity
UV	ultraviolet
x	characteristic length
Greek:	
β	air volume expansion coefficient
μ	air dynamic viscosity
ρ	air density
ν	air kinematic viscosity

1. INTRODUCTION

As of December 2020, viral infections continue to rise in New Mexico, and across most of the US. The vast majority of office rooms and commercial work spaces were not designed with viral mitigation in mind. In addition, new devices that help mitigate bio-aerosol viruses have appeared in the market. It is therefore of utmost importance to conduct bio-aerosol computational fluid dynamics (CFD) simulations to investigate flow patterns within work spaces, to evaluate the mitigation efficacy of building operation strategies and building designs, and to investigate recent advances in bio-aerosol mitigation devices; this set of modeling and validation priorities and strategies will be at the forefront of a leveraged NMSBA proposal in early 2021.

However, as a starting point, Bright Holdings, LLC desires a set of CFD simulations for suspended bio aerosol particles and architectural renderings to evaluate bio-aerosol mitigation technologies. The simulations are intended to provide design optimization insights with respect to Bright Holdings' bio aerosol mitigation devices, as well as building operational strategies for the reduction of bio aerosols. To that effect, the CFD goal was to simulate the dispersal of bio aerosols within an office/business environment. Given the project size of about 3.5 man weeks, it was decided to focus on a 'typical' hotel room, given its evident business environment connection and its similarities to work office spaces. Therefore, a CFD model was developed for a 'typical' hotel room unit consisting of a bedroom and bathroom. The hotel room configuration is described in detail in Section 2.

Three key simulations were conducted:

1) both the bathroom vent and HVAC were on,

2) only the HVAC was on,

and

3) only the bathroom vent was on.

The CFD model is described in Section 2, while the simulation assumptions and output are discussed in Section 3. Section 4 includes a discussion and summary of key insights and recommendations, as well as a discussion of models that can be considered under a larger analysis scope.

2. HOTEL ROOM MODEL

The full-scale CFD model includes items found in a 'typical' hotel room, including geometry, furnishings, and vents, as shown in Figure 2-1. In particular, the model includes an interconnected bedroom and bathroom. The bedroom includes a work desk, a bed, a storage closet, a window on the north side, and a heating, ventilation, and cooling (HVAC) unit on the north side. For convenience, the figure shows that the floor plan's top and bottom are oriented towards the north and south directions, respectively, while the left hand side (LHS) faces the west and the right hand side (RHS) points to the east, respectively. The bathroom includes a tub, a vanity wash basin, a toilet, an open entry way that links the bathroom to the bedroom, and a bathroom vent on the ceiling, right above the toilet. The hotel includes an entry door on the southeast corner, as well as a ½" vent gap at the bottom of the door. The door gap provides an important flow path, as will be shown in Section 3.

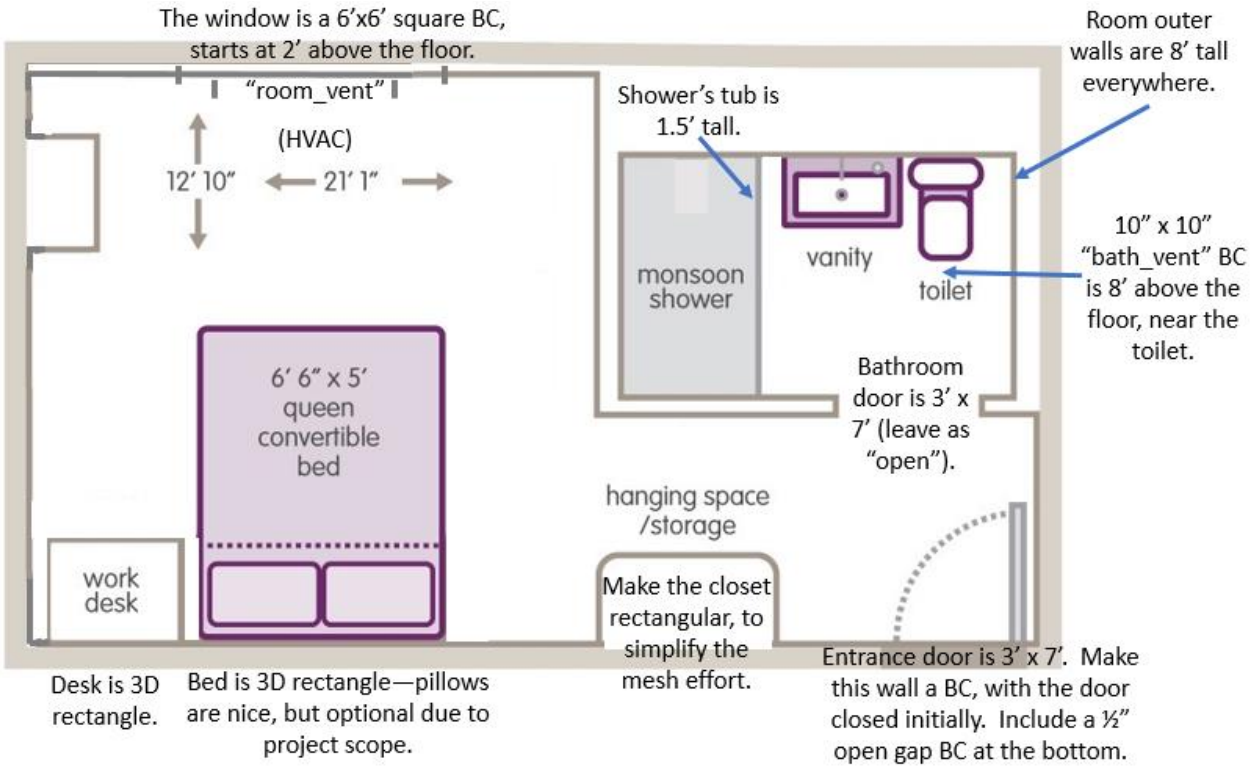

Figure 2-1. Hotel room floor plan.

The hotel room walls are 8' tall, while the bathroom and entry doors are both 3'x7'. The window, bathroom vent, and HVAC vent are 6'x6', 10"x10", and 4'x6", respectively. A top view of the CFD model is shown in Figure 2-2. Figure 2-3 shows the model from a tilted southwestern direction, with the southern and western walls removed for viewing convenience. Figure 2-4 shows the model from a tilted southeastern direction, with the southern and eastern walls removed for viewing convenience.

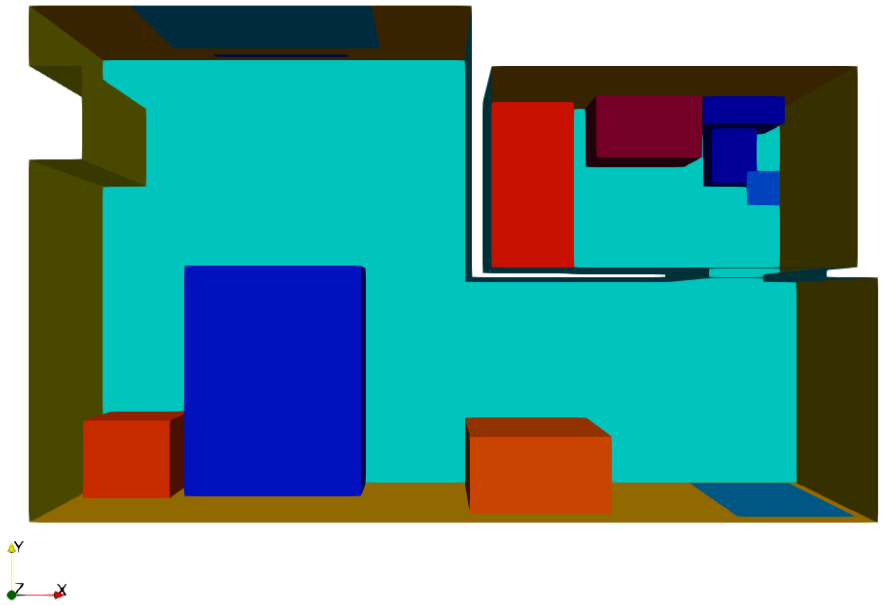

Figure 2-2. Top view of CFD hotel room model.

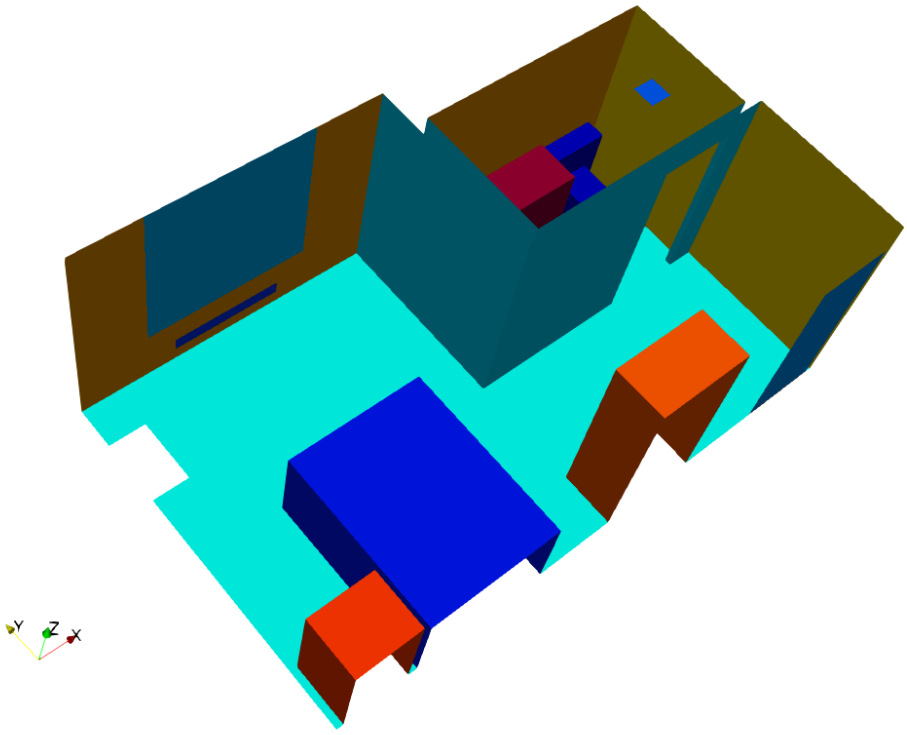

Figure 2-3. Southwestern view of CFD hotel room model

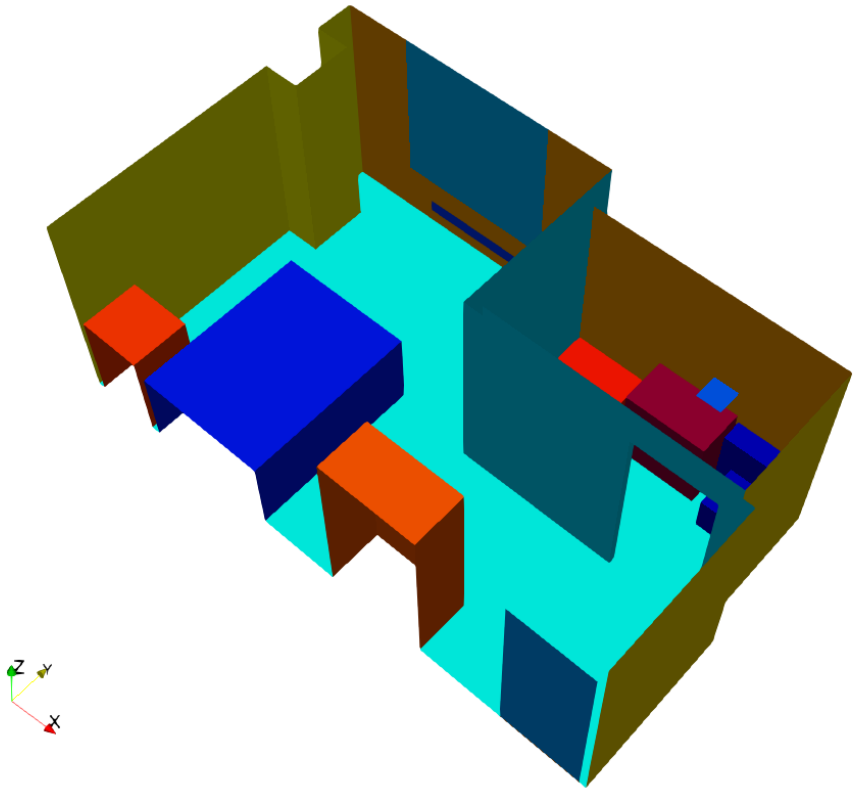

Figure 2-4. Southeastern view of CFD hotel room model.

Note that the HVAC is 6" above the floor, while the window is 2' above the floor. When active, the HVAC and bathroom vents operate at 0.5 and -0.5 m/s. In the case of the bathroom vent, the velocity is negative because the air flow is an outflow, while the HVAC velocity is positive because it is an inflow. Using conservation of mass arguments to assess the relative mass flow differences between the HVAC and the bathroom vent, the steady-state mass flow rate is defined as

$$1A) \quad \dot{m} = \rho u A$$

where

$\dot{m}$ = mass flow rate,

ρ = fluid density,

u = fluid velocity,

and

A = flow area.

Given that the bathroom and bedroom air have the same air density and velocity magnitude for this situation, *Equation 1A implies that the HVAC mass flow rate is much larger than the bathroom vent*. That is, the ratio of the mass flow rate between the HVAC and bathroom vents equals the ratio of the HVAC and bathroom flow areas,

$$1B) \quad \frac{\dot{m}_{HVAC}}{\dot{m}_{bathroom}} = \frac{\rho_{HVAC} |u_{HVAC}| A_{HVAC}}{\rho_{bathroom} |u_{bathroom}| A_{bathroom}} = \frac{A_{HVAC}}{A_{bathroom}}$$

Therefore, the mass flow rate from the HVAC greatly exceeds that of the bathroom vent for this particular situation; consequently, the excess mass flow rate results in an outflow through the ½" door gap.

Note that the entry door and windows can be opened or closed as desired, to investigate additional flow paths. In addition, the HVAC and bathroom vent velocities can be easily adjusted in the CFD model.

All model simulations used the Sandia National Laboratories Fuego CFD code, which is appropriate for incompressible flows up to Mach 0.7 or less. Fuego computes the coupled mass, momentum, and energy conservation equations. The code is fully implicit, so it is always computationally stable. For turbulent flows, the dynamic Smagorinsky large eddy simulation (LES) model was used [Wilcox, 2006; Rodriguez, 2019]. The LES model allows for the dynamic simulation of the integral and Taylor eddies that are generated primarily from the vents [Wilcox, 2006; Rodriguez, 2019]. In this case, the integral and Taylor eddies are simulated as they are born, cascade, and dissipate as a function of space and time throughout the system. The dynamic Smagorinsky model was selected because of its superb ability to model low to high Reynolds number (*Re*) flows, high swirl, and flow around obstacles; the standard k-ε model was not employed because of its inability to adequately model these flow conditions [Rodriguez, 2019]. The momentum equation was coupled to the energy equation using the Boussinesq approximation. Thus, the hotel room CFD model is suitable for natural circulation flow, mixed flow, and forced flow. Natural circulation flow occurs when all vents are off and the window and doors are closed, so the flow is purely the result of fluid density differences resulting from the temperature gradients in the room walls, windows, and other structures. Forced flows include the HVAC, bathroom vent, fans, and wind (if any).

Care was taken that the computational meshes had sound, "bullet proof" mesh metrics as found in the literature [Rodriguez, 2019]. These metrics include the aspect ratio, skew, scaled Jacobian, and the growth ratio between adjacent elements. In addition, the "dice" meshing technique was used to provide a boundary layer with three fine elements with radial biasing. A highly-recommended set of mesh metrics was employed, using the following "grail" (gold standard) mesh metric group [Rodriguez, 2019]:

- Aspect ratio ≤ 5
- Skew ≤ 0.5
- Expansion ratio ≤ 1.5
- Scaled Jacobian ≥ 0.5

For fast test-out of the models, a coarse mesh with 0.406 million elements was developed. As confidence with the model increased, medium and fine meshes were generated with 2 and 7.5 million elements, respectively. Certainly, finer mesh resolution could be used, but given the project scope and timeline, the medium and fine meshes generated reasonably-converged spatial solutions. An added benefit of the meshes was that the simulations could be completed within three to eight hours using 64 to 128 parallel processors. If the project advances in 2021, higher-resolution meshes will require several thousand processors, which is well within Sandia's high performance computational capacity.

3. COMPUTATIONAL FLUID DYNAMICS SIMULATIONS

Re and the Grashof number (*Gr*) were considered as a guide for the development of the CFD models. In particular, *Re* measures the relative impact of turbulence and heat transfer during forced flow, and is defined as,

$$2)\ Re = \frac{x_{char} u_{char} \rho}{\mu} = \frac{x_{char} u_{char}}{\nu}$$

where

x_{char} = flow channel characteristic length,

u_{char} = fluid characteristic velocity,

ρ = fluid density,

μ = fluid dynamic viscosity,

and

$\nu = \frac{\mu}{\rho}$ = fluid kinematic viscosity.

For natural circulation flows, the magnitude of the dimensionless Grashof number (*Gr*) dictates the degree of convection heat transfer during flows induced by temperature gradients. Thus, the fluid moves as a result of the density differences associated with variations in system temperature. *Gr* times the Prandtl number (*Pr*) is a measure of the degree of laminarity or turbulence under natural circulation, where *GrPr* = Rayleigh number = *Ra* [Holman, 1990; Rodriguez, 2019]. *Gr* is defined as,

$$3)\ Gr = \frac{\beta g h^3 \Delta T}{\nu^2}$$

where

$\Delta T = (T_w - T_\infty)$,

T_w = wall temperature,

T_∞ = fluid temperature far away from the heat transfer wall,

β = fluid volume expansion coefficient,

g = gravitational constant,

and

h = system characteristic height.

For turbulent natural circulation flows over a vertical plate [Holman, 1990],

$$4)\ Nu = 0.1(GrPr)^{1/3}$$

The Boussinesq approximation was used to couple the conservation of momentum and energy equations to model the buoyant, natural circulation flow; that is,

$$5A)\ \rho\frac{\partial u}{\partial t} = -\rho\left(u\frac{\partial u}{\partial x} + \mathrm{v}\frac{\partial u}{\partial y} + w\frac{\partial u}{\partial z}\right) + \mu\left(\frac{\partial^2 u}{\partial x^2} + \frac{\partial^2 u}{\partial y^2} + \frac{\partial^2 u}{\partial z^2}\right) + g_x\left(\rho_\infty - \rho\right)$$

$$= -\rho\left(u\frac{\partial u}{\partial x} + \mathrm{v}\frac{\partial u}{\partial y} + w\frac{\partial u}{\partial z}\right) + \mu\left(\frac{\partial^2 u}{\partial x^2} + \frac{\partial^2 u}{\partial y^2} + \frac{\partial^2 u}{\partial z^2}\right) + \rho g_x\left[\beta\left(T - T_\infty\right)\right]$$

$$5B)\ \rho\frac{\partial \mathrm{v}}{\partial t} = -\rho\left(u\frac{\partial \mathrm{v}}{\partial x} + \mathrm{v}\frac{\partial \mathrm{v}}{\partial y} + w\frac{\partial \mathrm{v}}{\partial z}\right) + \mu\left(\frac{\partial^2 \mathrm{v}}{\partial x^2} + \frac{\partial^2 \mathrm{v}}{\partial y^2} + \frac{\partial^2 \mathrm{v}}{\partial z^2}\right) + g_y\left(\rho_\infty - \rho\right)$$

$$= -\rho\left(u\frac{\partial \mathrm{v}}{\partial x} + \mathrm{v}\frac{\partial \mathrm{v}}{\partial y} + w\frac{\partial \mathrm{v}}{\partial z}\right) + \mu\left(\frac{\partial^2 \mathrm{v}}{\partial x^2} + \frac{\partial^2 \mathrm{v}}{\partial y^2} + \frac{\partial^2 \mathrm{v}}{\partial z^2}\right) + \rho g_y\left[\beta\left(T - T_\infty\right)\right]$$

$$5C)\ \rho\frac{\partial w}{\partial t} = -\rho\left(u\frac{\partial w}{\partial x} + \mathrm{v}\frac{\partial w}{\partial y} + w\frac{\partial w}{\partial z}\right) + \mu\left(\frac{\partial^2 w}{\partial x^2} + \frac{\partial^2 w}{\partial y^2} + \frac{\partial^2 w}{\partial z^2}\right) + g_z\left(\rho_\infty - \rho\right)$$

$$= -\rho\left(u\frac{\partial w}{\partial x} + \mathrm{v}\frac{\partial w}{\partial y} + w\frac{\partial w}{\partial z}\right) + \mu\left(\frac{\partial^2 w}{\partial x^2} + \frac{\partial^2 w}{\partial y^2} + \frac{\partial^2 w}{\partial z^2}\right) + \rho g_z\left[\beta\left(T - T_\infty\right)\right]$$

In summary, laminar and turbulent circulation flows are considered in the analysis, under both natural and forced conditions.

3.1. Simulation with Both HVAC and Bathroom Vents On

The simulation with both HVAC and bathroom vents active is referred as the base case, and is shown in Figures 3-1 through 3-9 from 0 to 120 s, in 15 s intervals. Figure 3-1 shows the initial state at time 0 s. In particular, at 0 s, all vents are off and there is zero flow within the room. Then, both vents immediately become active upon initiation of the transient, so a dynamic situation ensues, whereby the bathroom vent begins outflowing the air adjacent to the bathroom area and the HVAC air begins flowing into the room. *Figure 3-2 shows the lower flow pattern streamlines from the HVAC at 15 s, when the flow finally reaches and exits through the entry door's lower gap, while the remaining HVAC upper flow pattern exits through the bathroom vent.* Note that streamlines are similar to the smoke lines observed in wind tunnels—these are the flow paths followed by the fluid. Figure 3-3 shows that by about 30 s, the flow pattern reaches a pseudo steady state, whereby the flow pattern oscillates about a mean flow velocity that is forced by the transient dynamics of the turbulent flow; the back and forth sloshing of the turbulent flow is readily observed by comparing Figures 3-3 through 3-9.

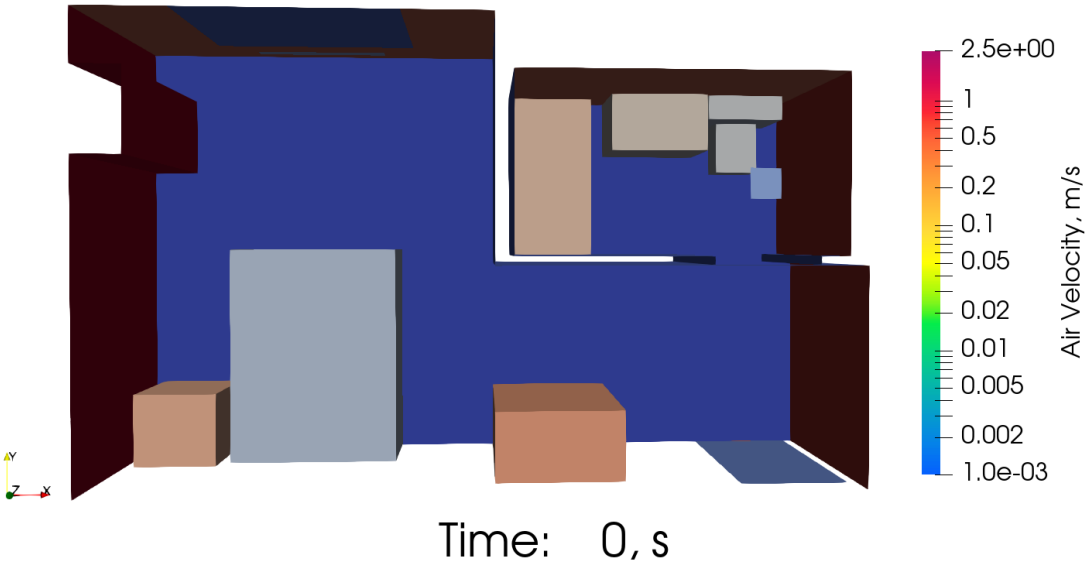

Figure 3-1. Velocity distribution at 0 s—Event Initiation.

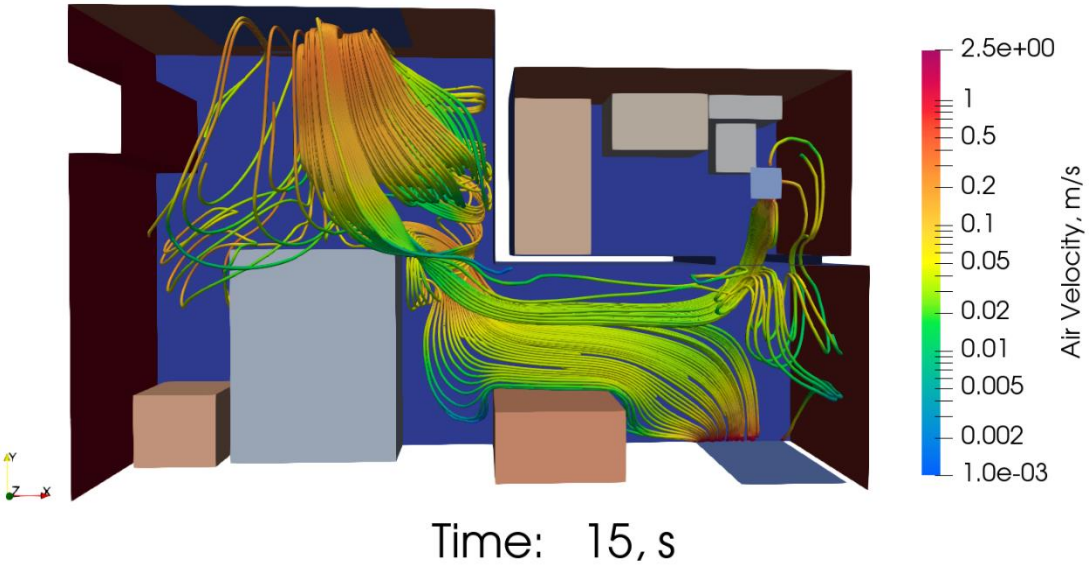

Figure 3-2. Velocity distribution at 15 s (HVAC flow reaches door gap).

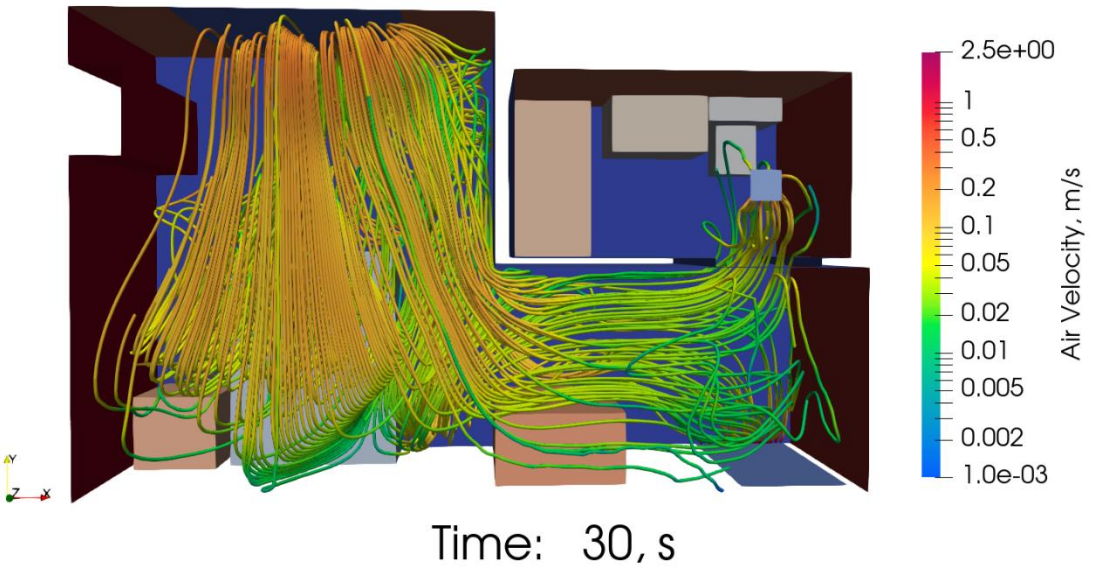

Figure 3-3. Velocity distribution at 30 s (the rooms reach a pseudo steady state).

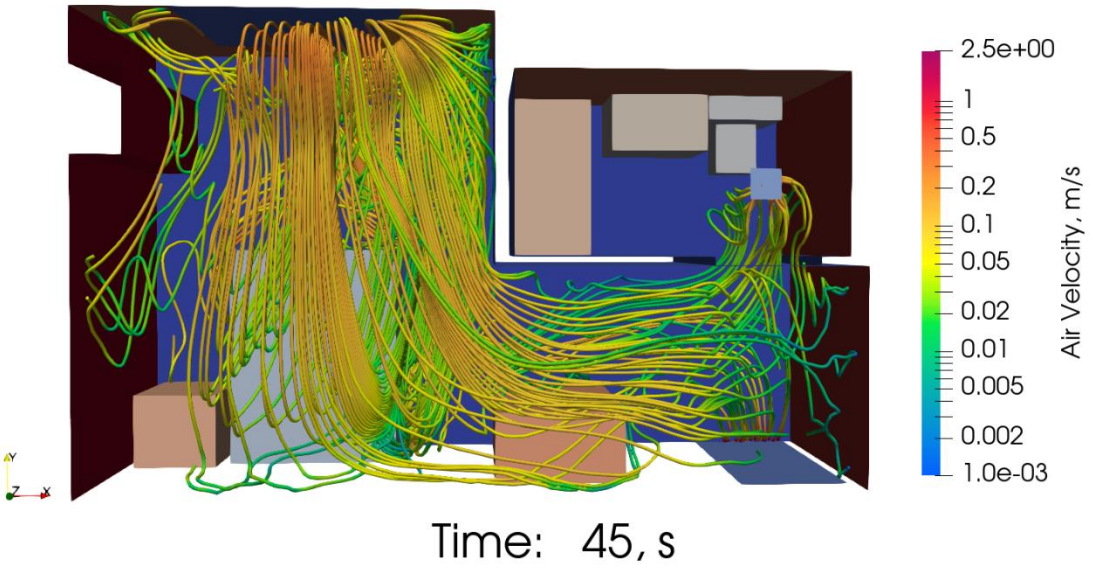

Figure 3-4. Velocity distribution at 45 s (flow oscillates about mean from 45 to 120 s).

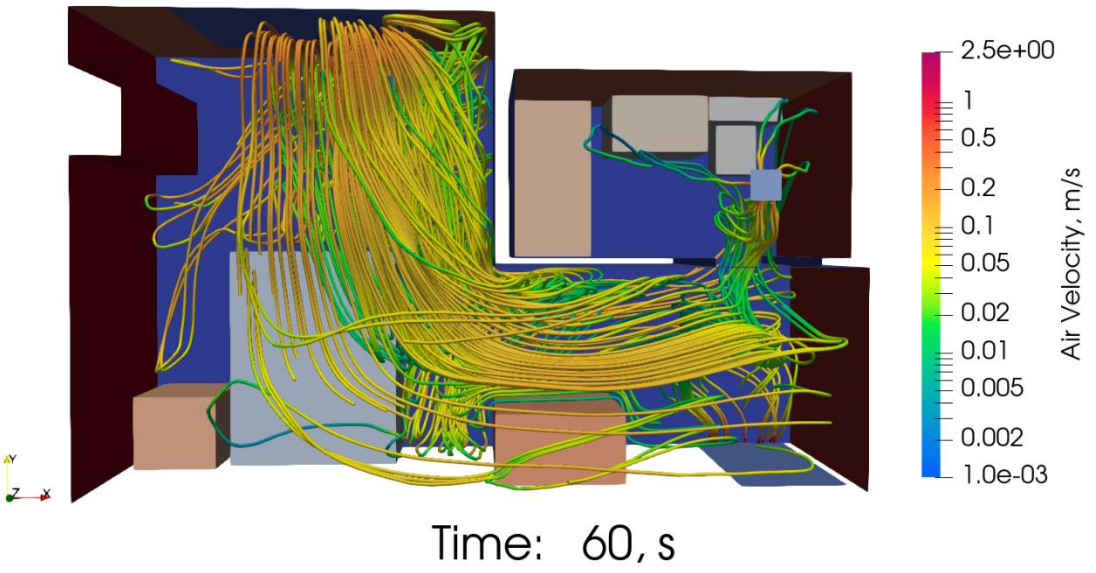

Figure 3-5. Velocity distribution at 60 s.

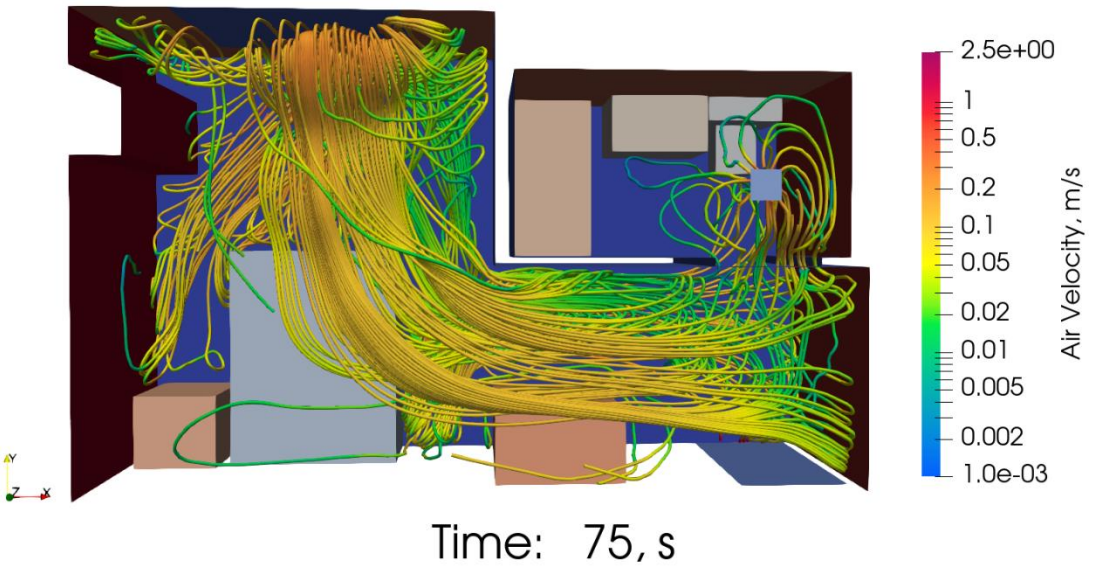

Figure 3-6. Velocity distribution at 75 s.

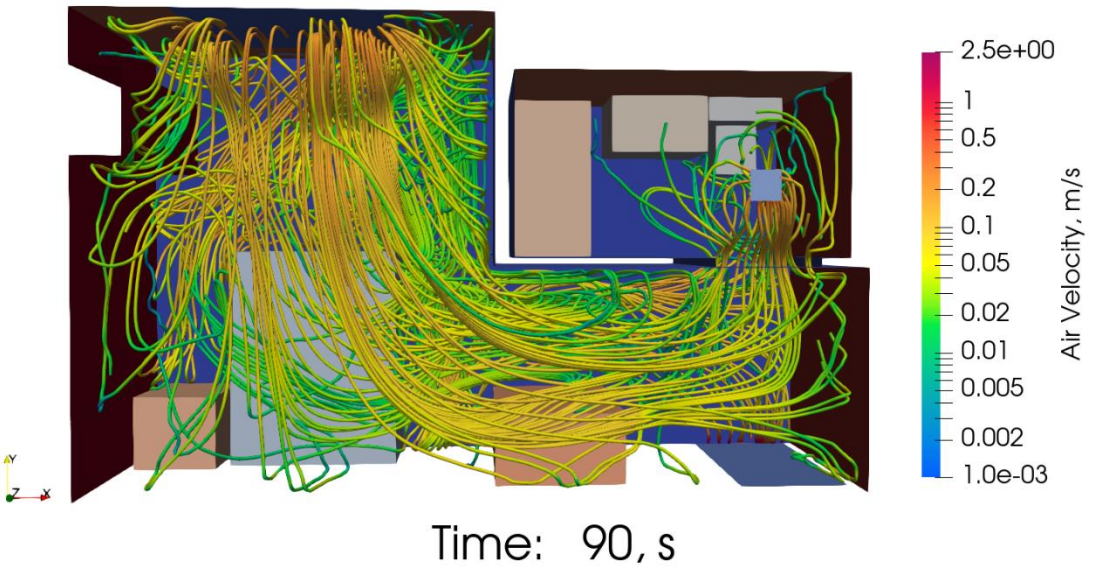

Figure 3-7. Velocity distribution at 90 s.

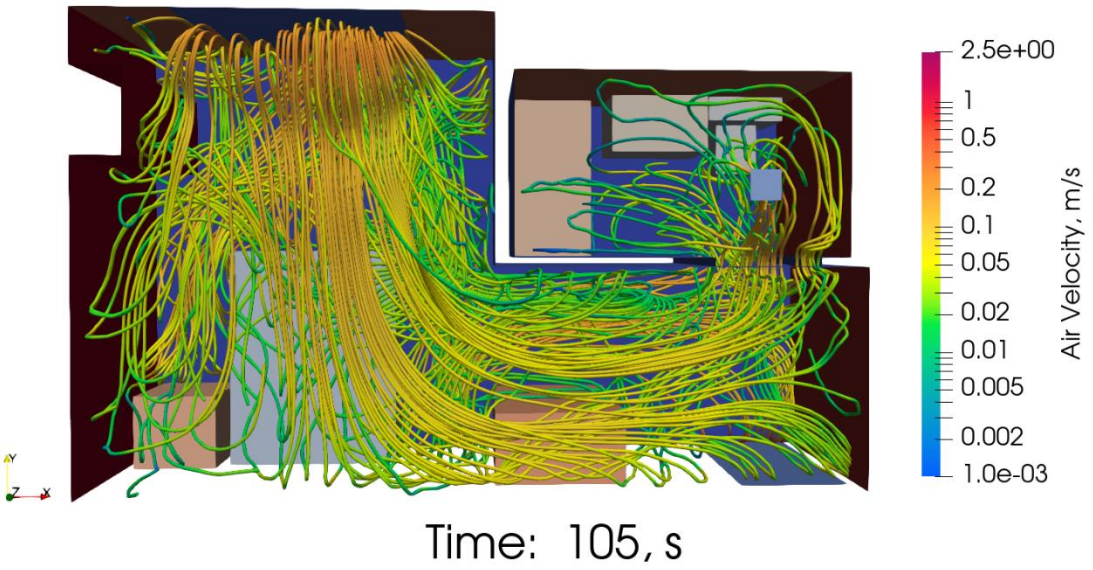

Figure 3-8. Velocity distribution at 105 s.

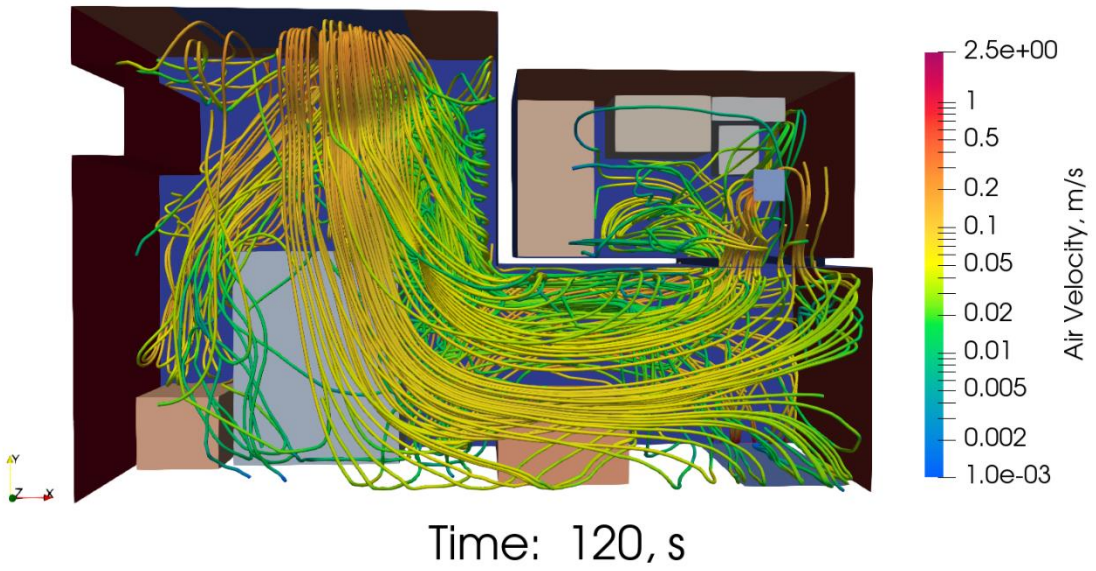

Figure 3-9. Velocity distribution at 120 s.

Figure 3-10 is the same as Figure 3-9, except that the image is now viewed from the southwestern side. For visualization convenience, the western and southern walls are removed. From this viewing frame of reference, it is easier to observe the recirculation pattern (similar to a roll), that is adjacent to the northern and western sides of the bed. *In essence, the flow recirculates in the region between the HVAC and the bed, and eventually splits into two upper and lower flow regions. The upper flow region proceeds onto the bathroom, and is exhausted by the bathroom vent. By contrast, the HVAC lower flow region proceeds to the ½" gap between the floor and the bottom of the entry door.*

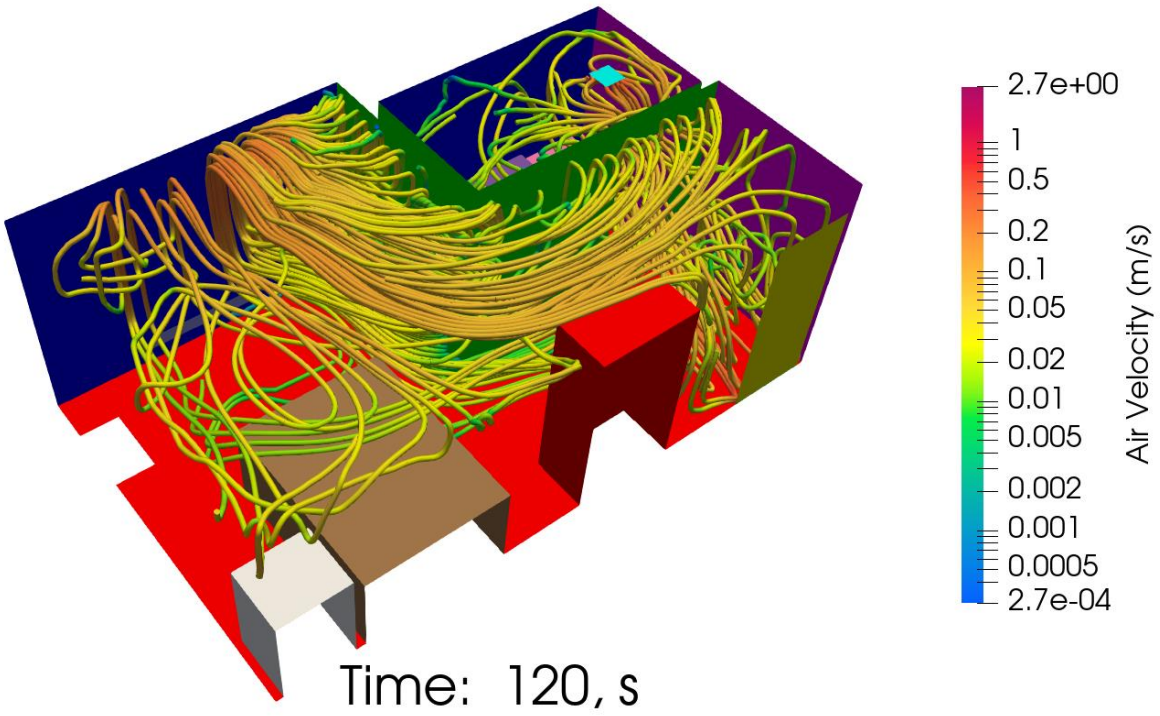

Figure 3-10. Velocity distribution at 120 s—southwestern view.

Again, for visualization convenience, Figure 3-9 is rotated to show the northwestern region shown in Figure 3-11. In this case, the north and west walls are removed to show the streamline velocity distribution from the northern side. *From the vantage point of Figures 3-10 and 3-11, it is easier to see the HVAC upper and lower recirculation patterns.*

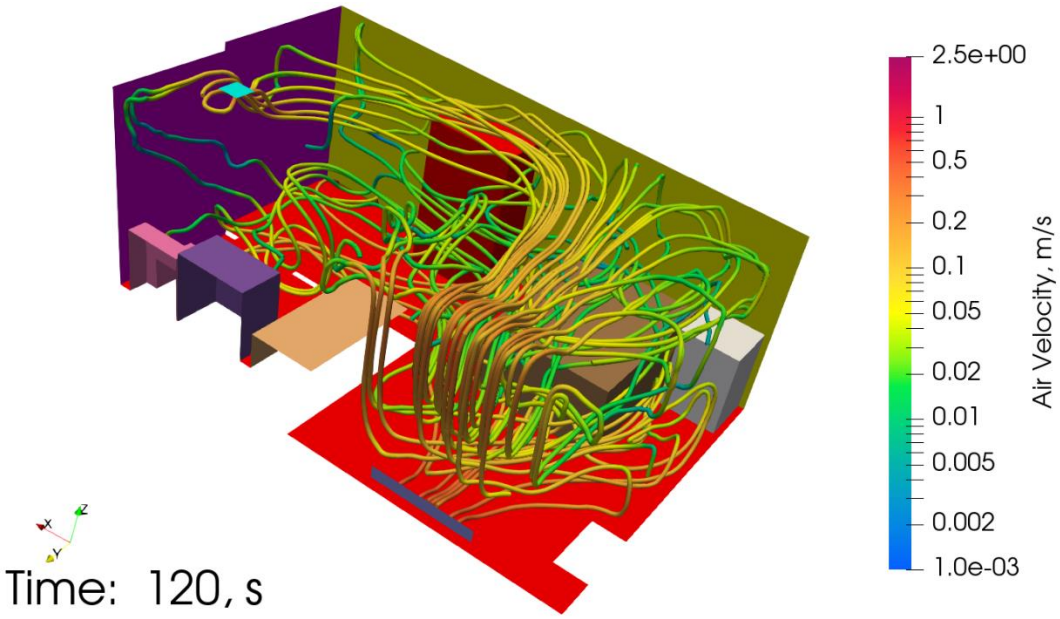

Figure 3-11. Velocity distribution at 120 s—northwestern view.

Instead of using streamlines, Figure 3-12 shows a southwestern view using velocity arrows, while Figure 3-13 shows the southeastern view.

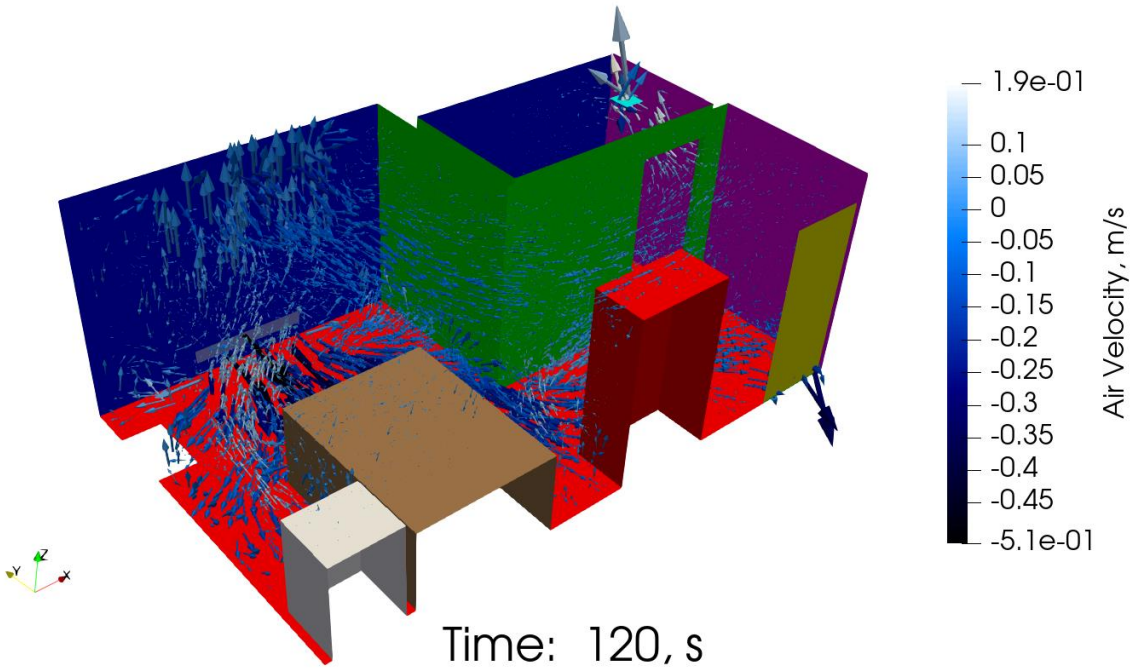

Figure 3-12. Velocity distribution at 120 s using arrows—southwestern view.

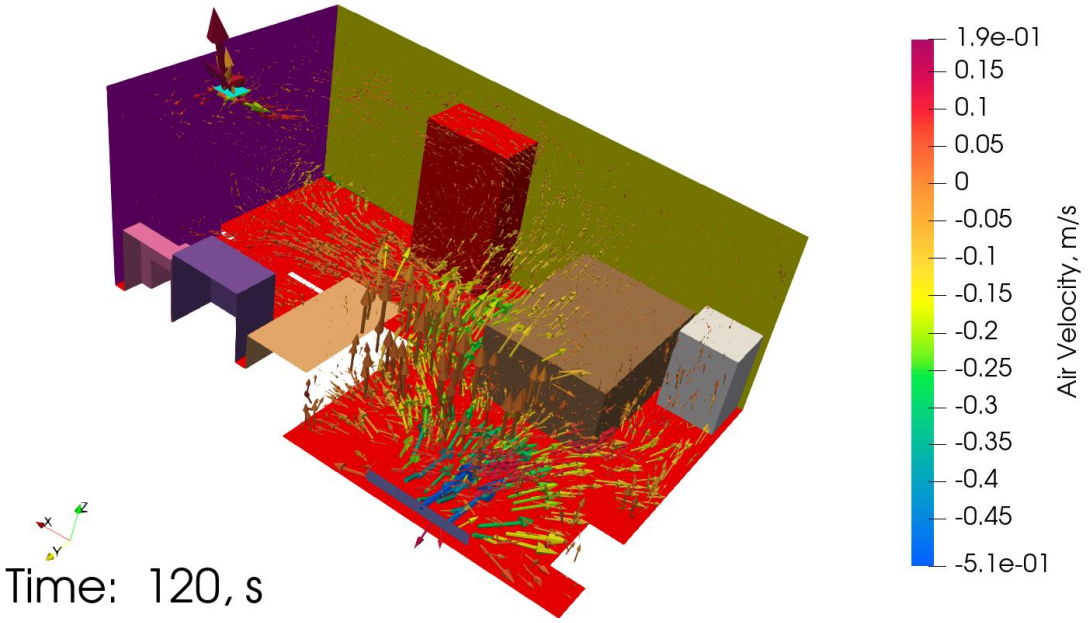

Figure 3-13. Velocity distribution at 120 s using arrows—southeastern view.

Figures 3-14 through 3-17 show the normalized total kinetic energy (TKE). TKE is a measure of the degree of turbulence. For these figures, 3D contours are shown in the normalized range from $1x10^{-6}$ to 1.0. The figures show TKE at 30 s intervals for the 120 s simulation. *Note that the TKE regions show where the highest degree of turbulent flow exists. Many of these regions include swirling eddy coherent structures that rotate and break as they disperse throughout the rooms. As expected and shown by the figures, these structures tend to occur in recirculation areas and corners. These are the regions where recirculation and swirling would tend to accumulate the largest concentrations of airborne particles, pathogens, dust, etc. In particular, these regions are analogous to sinuous river beds, where certain regions concentrate heavier particles, such as gold, as a result of turbulent swirling recirculation.*

In summary, the simulation shows complex flow patterns with distinct upper and lower flow regions, swirling flow, and significant levels of turbulent mixing. These provide intriguing insights that can be exploited to help mitigate pathogen aerosol dispersion, provide building design guidelines, as well as generate insights for the strategic placement of mitigation devices, such as ultraviolet (UV) light, supplemental fans, and filters.

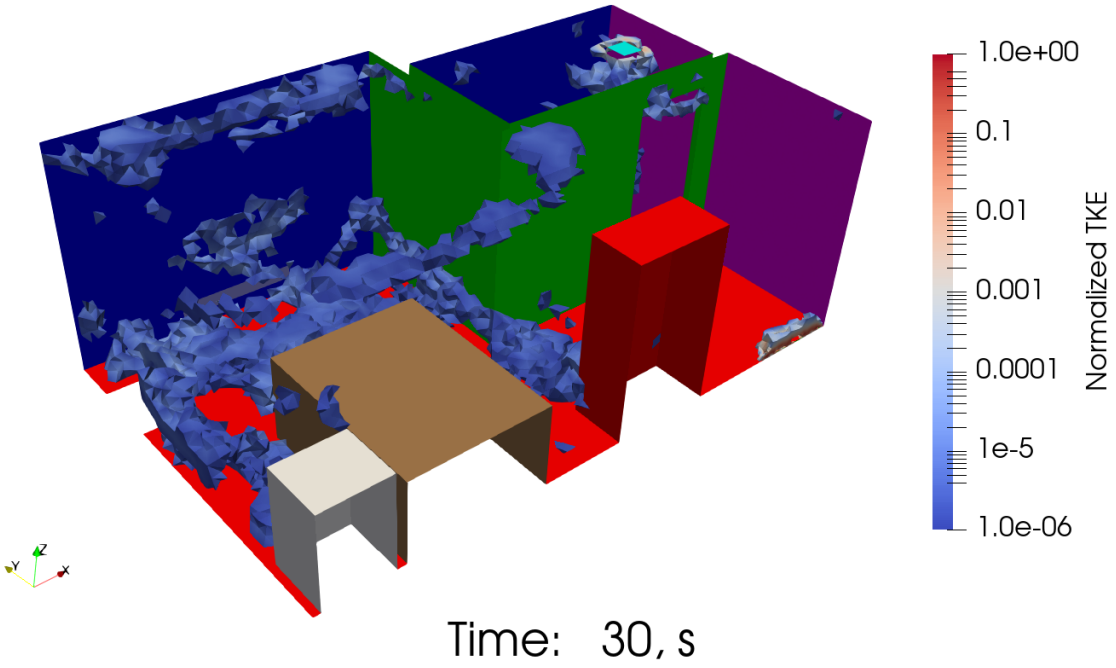

Figure 3-14. Normalized TKE at 30 s.

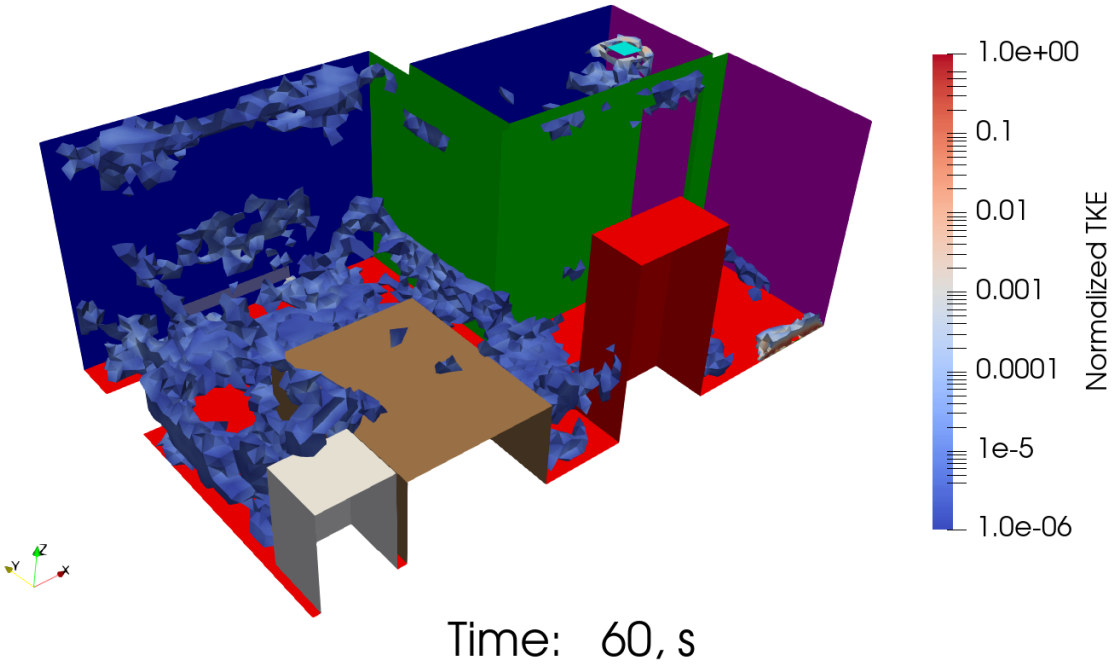

Figure 3-15. Normalized TKE at 60 s.

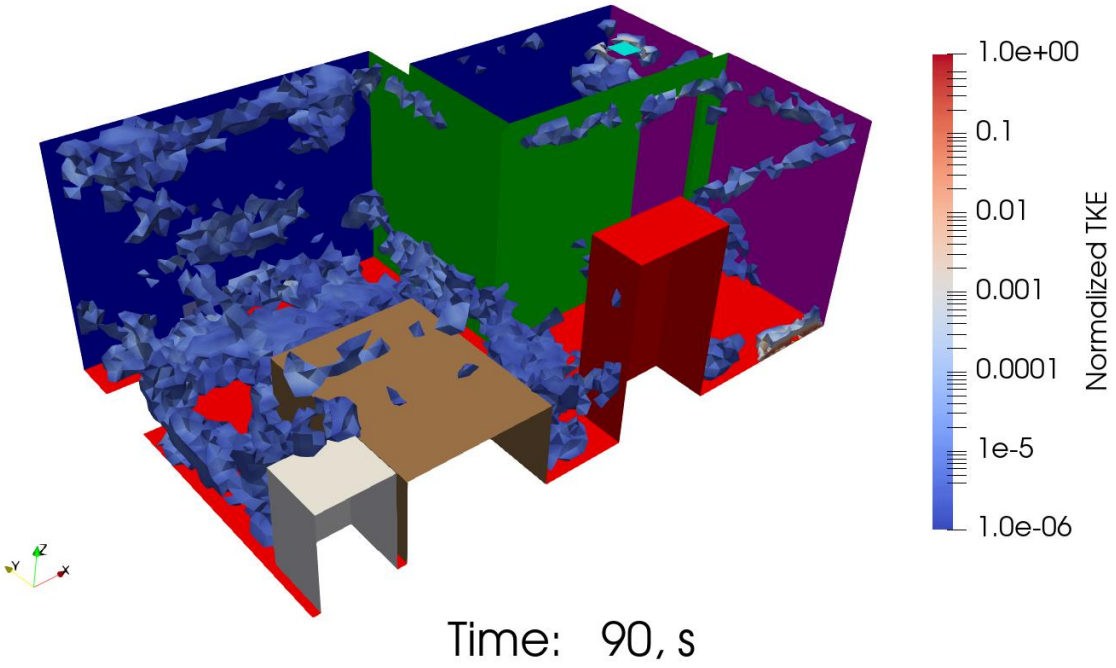

Figure 3-16. Normalized TKE at 90 s.

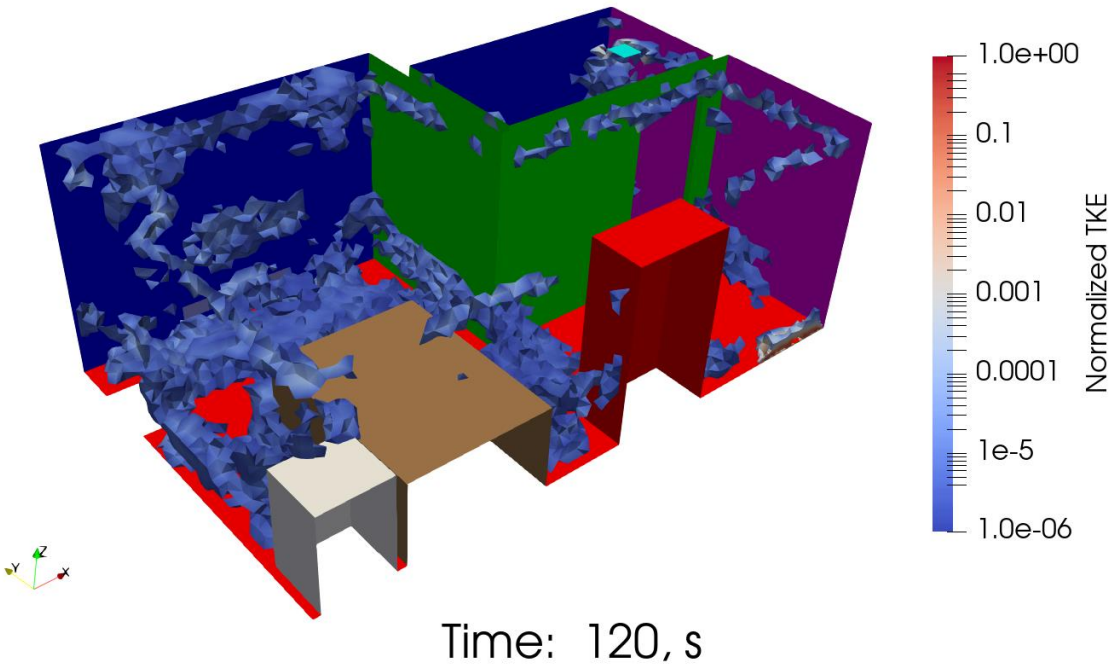

Figure 3-17. Normalized TKE at 120 s.

3.2. Simulation with Only the HVAC Vent On

For this simulation, the HVAC was on, but the bathroom vent was off. The velocity streamlines at 120 s are shown in Figure 3-18, which shows a view from the top. Figure 3-19 shows the same time interval, but from the southwestern side. *The primary difference between this simulation and the one presented in Section 3.1 (the base case) is that the HVAC upper region air flows into the bathroom, where it recirculates, until it finally exits through the door gap. If the HVAC air is from a fresh, clean source, or passes through a filter/UV device, then this bathroom recirculation is innocuous. However, if the HVAC air is shared with other guest rooms and recirculated without mitigation mechanisms, then the airborne particles will simply recirculate in the bathroom, causing potential issues when the bathroom is occupied.*

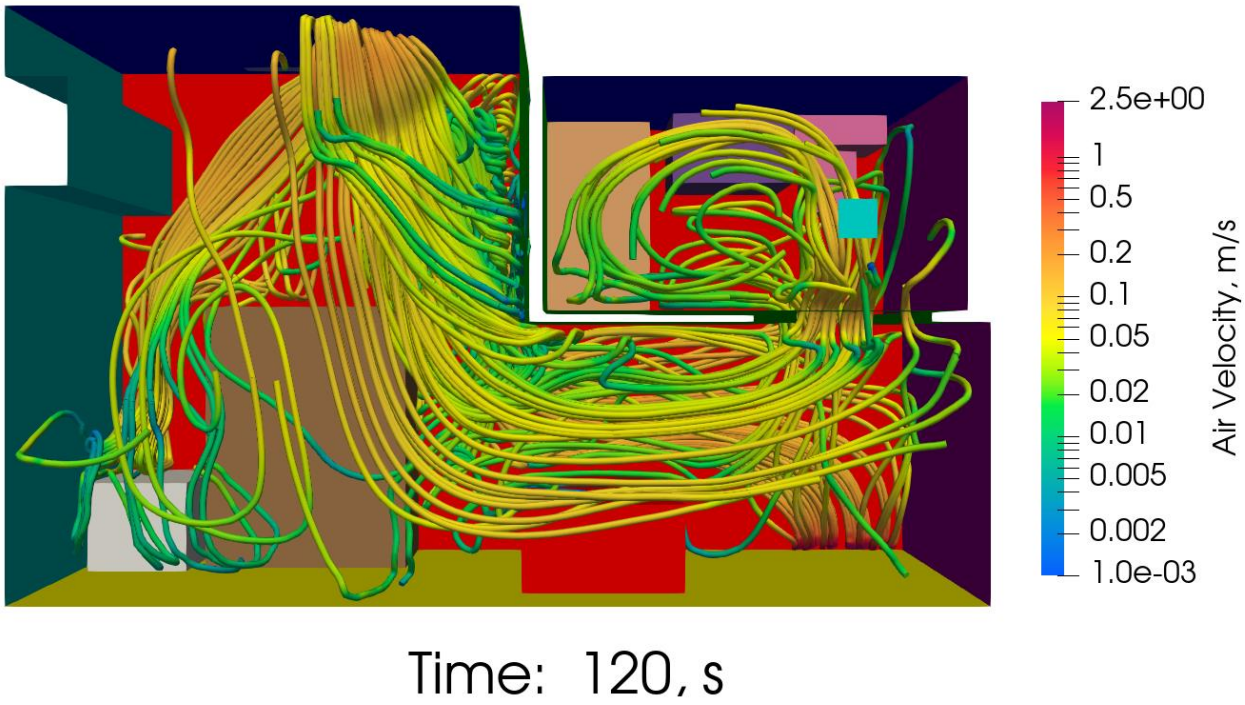

Figure 3-18. Velocity distribution at 120 s—only the HVAC is on; top view.

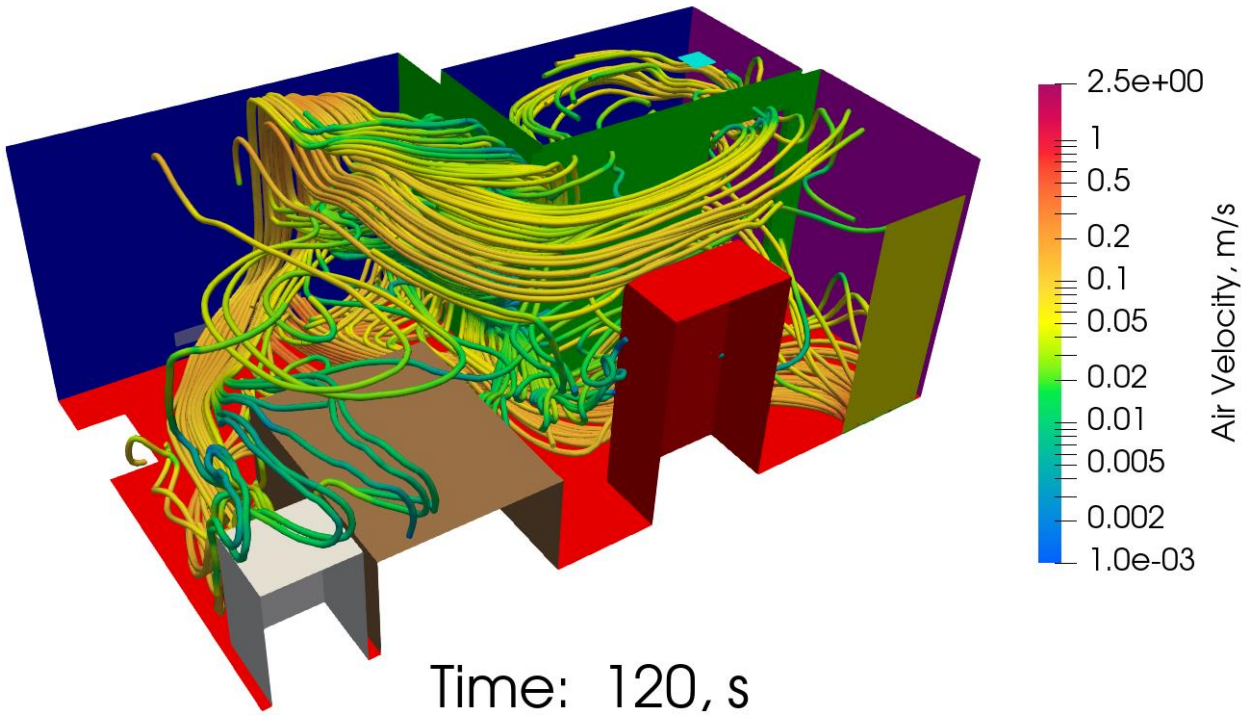

Figure 3-19. Velocity distribution at 120 s—only the HVAC is on; southwestern view.

3.3. Simulation with Only the Bathroom Vents On

Finally, the bathroom vent was on, but the HVAC was off. The velocity streamlines at 120 s are shown in Figure 3-20, which shows a view from the top. Figure 3-21 shows the same interval, but from the southwestern side. *Because the bathroom vent is an air sink, airborne particles exit the bathroom.* Notice that very little air flow occurs within the first half of the bedroom north western region as a result of a small degree of induced recirculation. *The primary difference between this simulation and the one presented in Section 3.1 (the base case) is that the bathroom vent induces an* ***inflow*** *at the door entrance. However, the vent-induced flow generates a suction that brings air into the room through the ½" door gap; air coming from the hallway can be of dubious origin, so this configuration should be avoided.*

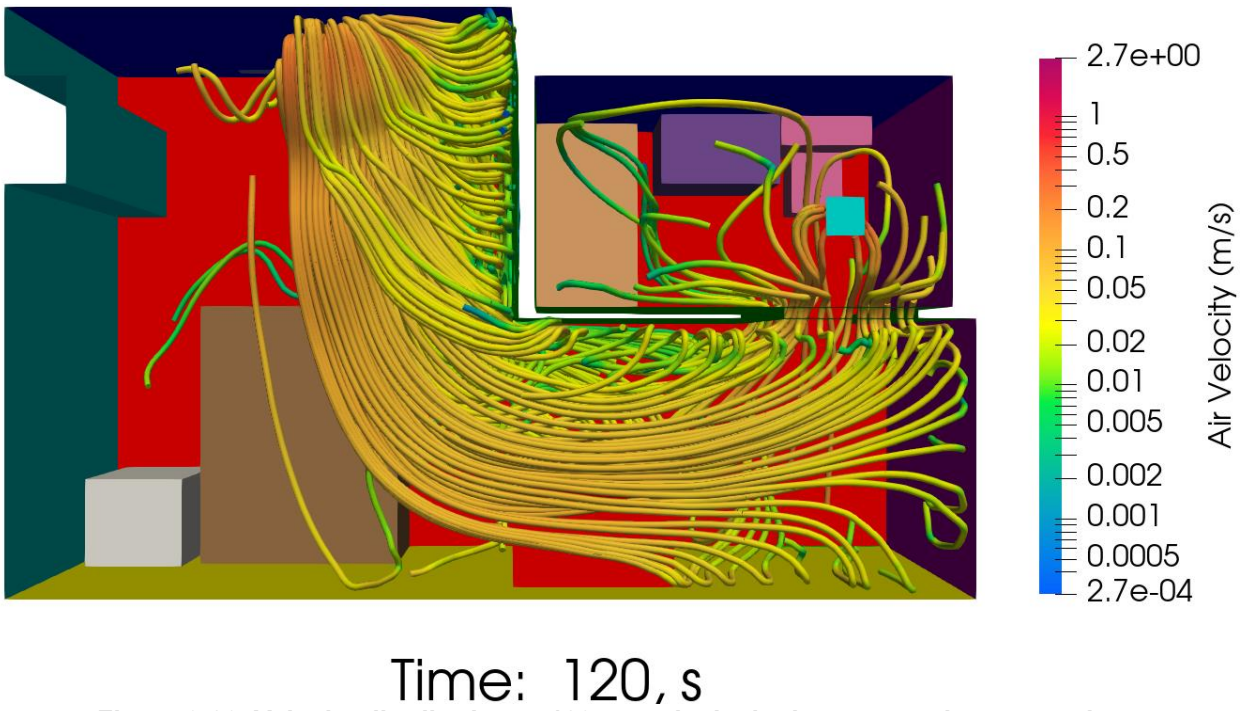

Figure 3-20. Velocity distribution at 120 s—only the bathroom vent is on; top view.

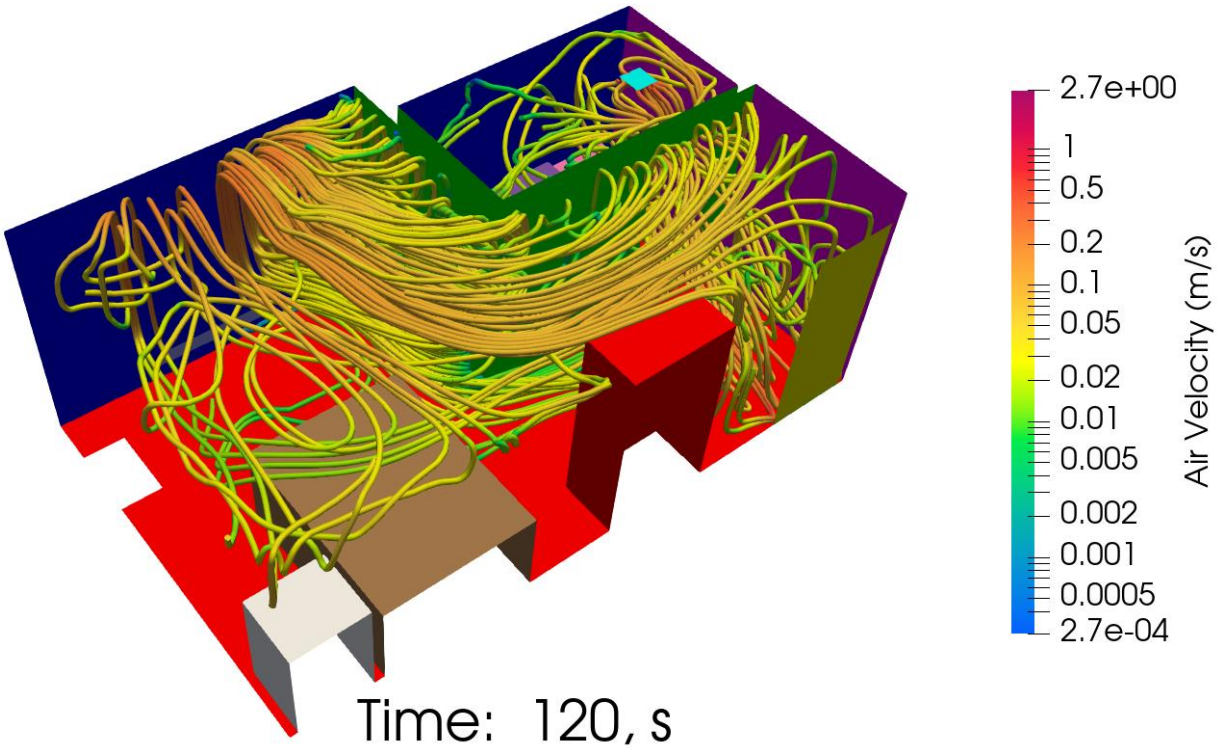

Figure 3-21. Velocity distribution at 120 s—only the bathroom vent is on; southwestern view.

4. SUMMARY, KEY FINDINGS AND RECOMMENDATIONS, AND SUGGESTIONS FOR FUTURE WORK

A full scale 'typical' configuration for a hotel room with a bathroom and bedroom was modeled using CFD. The simulation shows complex flow patterns with distinct upper and lower flow regions, swirling flow, and significant levels of turbulent mixing. These provide intriguing insights that can be exploited to help mitigate pathogen aerosol dispersion, generated building design guidelines, as well as provide insights for the strategic placement of mitigation devices, such as ultraviolet (UV) light, supplemental fans, and filters.

- Three key simulations were conducted:
  - both the bathroom vent and HVAC were on,
  - only the HVAC was on, and
  - only the bathroom vent was on.
- The HVAC mass flow rate was much larger than the bathroom vent, meaning that the excess mass flow rate generates an outflow through the ½" entry door gap near the floor. This is a safe configuration *if the HVAC air is from a fresh, clean source, or passes through a filter/UV device.*
- When the HVAC and bathroom vents are on, two distinct flow patterns are generated. In particular, the flow recirculates in the region between the HVAC and the bed, until it splits into lower and upper regions. The lower region passes through the bottom of the bedroom and exits through the ½" gap between the entry door and the floor. The upper region pattern passes through the upper part of the bedroom and exits through the bathroom vent.
- When the HVAC is on, but the bathroom vent is off, the HVAC upper region air flows into the bathroom, where it recirculates, until it finally exits through the door gap. *If the HVAC air is from a fresh, clean source, or passes through a filter/UV device, then this bathroom recirculation is innocuous. However, if the HVAC air is shared with other guest rooms and recirculated without mitigation mechanisms, then the airborne particles will simply recirculate in the bathroom, causing potential issues when the bathroom is occupied.*
- When the HVAC is off, but the bathroom vent is on, the bathroom vent induces an **inflow** at the door entrance. *Unfortunately, the vent-induced flow generates a suction that brings air into the room through the ½" door gap; air coming from the hallway can be of dubious origin, so this configuration should be avoided.*
- Note that the TKE regions show where the highest degree of turbulent flow exists. Many of these regions include swirling eddy coherent structures that rotate and break as they disperse throughout the rooms. Most importantly, these are the regions where recirculation and swirling tend to accumulate the largest concentrations of heavier airborne particles, pathogens, dust, etc. *Thus, regions with the largest TKE tend to occur in areas with flow recirculation and corners, so this presents a reasonable metric to guide the strategic location of pathogen mitigation devices.*

Future work in this area will benefit from the following:

- Additional CFD simulations to consider additional geometries and operational configurations.
- Additional models can be included, through Fuego and other Sandia tools, such as MELCOR. In conjunction, these models can include transport, gravitational settling, resuspension, attachment, hygroscopicity, and agglomeration.
- In addition, the models can include filter, vent, and UV irradiation models.

- Scaled aerosol experiments using safe bio aerosol simulants.
- The experiments can help validate the bio aerosol mitigation devices and CFD simulations.

This page left blank

REFERENCES

Fuego Theory Manual, "SIERRA/Fuego Theory Manual – 4.11", Draft, Sandia National Laboratories, 2009A.

Fuego User's Manual, "SIERRA/Fuego User's Manual – 4.14", SAND 2006-6084P, Sandia National Laboratories, 2009B.

Holman, J. P., Heat Transfer. McGraw-Hill, Seventh Edition, New York, 1990.

Rodriguez, S., *Applied Computational Fluid Dynamics and Modeling—Practical Tools, Tips, and Techniques*, Springer Publishing, 2019.

Wilcox, D. C., *Turbulence Modeling for CFD*, 3rd Ed., DCW Industries, Inc., 2006.

DISTRIBUTION

Email—Internal

Name	Org.	Sandia Email Address
Technical Library	01977	sanddocs@sandia.gov

Email—[redacted]

Name	Company Email Address	Company Name
Issac Barboza	Barbosa@neat.energy	Bright Holdings, LLC
Patrick Ruiz	pat@neat.energy	NEAT Energy

This page left blank

Sandia National Laboratories

Sandia National Laboratories is a multimission laboratory managed and operated by National Technology & Engineering Solutions of Sandia LLC, a wholly owned subsidiary of Honeywell International Inc. for the U.S. Department of Energy's National Nuclear Security Administration under contract DE-NA0003525.